Journal of Power Sources 262 (2014) 183–191

Contents lists available at ScienceDirect

Journal of Power Sources

journal homepage: www.elsevier.com/locate/jpowsour

Bioelectro-catalytic valorization of dark fermentation effluents by acetate oxidizing bacteria in bioelectrochemical system (BES)

Ahmed ElMekawy [a,b,1], Sandipam Srikanth [b,1], Karolien Vanbroekhoven [b], Heleen De Wever [b], Deepak Pant [b,*]

[a] Genetic Engineering and Biotechnology Research Institute, University of Sadat City (USC), Sadat City, Egypt
[b] Separation and Conversion Technology, VITO – Flemish Institute for Technological Research, Boeretang 200, Mol 2400, Belgium

HIGHLIGHTS

- An MFC was operated with enriched biocatalyst from farm manure.
- Utilizing dark fermentation effluents as primary substrate in MFC.
- Bioelectrochemical analysis along with the wastewater treatment was studied.
- Shifts in organic acid contents during the process were linked to power output.
- Fraction of COD converted to power was calculated and compared with literature.

GRAPHICAL ABSTRACT

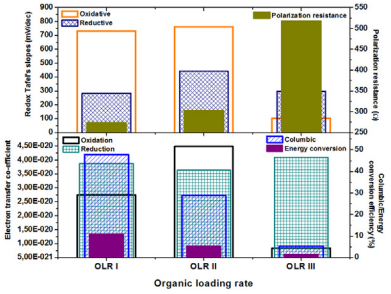

ARTICLE INFO

Article history:
Received 22 November 2013
Received in revised form
3 March 2014
Accepted 24 March 2014
Available online 1 April 2014

Keywords:
Bioelectrochemical system (BES)
Wastewater treatment
Dark fermentation
Cattle manure
Organic load
Microbial fuel cell (MFC)

ABSTRACT

Biovalorization of dark fermentation effluent (DFE) in a microbial fuel cell (MFC) was studied using the biocatalyst enriched from farm manure. The MFC performance was evaluated in terms of power density, substrate degradation, energy conversion efficiency and shifts in system redox state with operation time and organic loading rate (OLR). Higher power density of 165 mW m^{-2} (12.5 W m^{-3}) was observed at OLR I, which dropped to 86 mW m^{-2} at OLR II and 39 mW m^{-2} at OLR III. The substrate degradation was also higher at OLR I (72%) and diminished with increasing the OLR. The pH showed rapid drop and fluctuations initially when shifted to DFE but adapted over time. Higher coulombic efficiency was observed (48% at OLR I) contributing to a total energy conversion of 11%, which is higher compared to the available literature. However, the MFC performance declined at higher OLR with respect to all the performance indicators. DFE consisted of residual sugars from first stage process along with the volatile fatty acids (VFAs) and alcohols, which contributed for the generation of organic acids with their simultaneous consumption and led to VFA increment in spite of COD removal. Cyclic voltammograms along with the derived electro-kinetics supported the observed shifts.

1. Introduction

The current energy crisis and the resulting price escalations have drawn considerable attention toward the exploration of alternative eco-friendly renewable energy sources [1]. The biological production of hydrogen from waste organics has attracted the global attention as a clean energy source and a potential alternative

* Corresponding author. Tel.: +32 14 33 6969; fax: +32 14 326586.
E-mail addresses: deepak.pant@vito.be, pantonline@gmail.com (D. Pant).
[1] These authors equally contributed to this paper and should be both considered as co-first authors.

http://dx.doi.org/10.1016/j.jpowsour.2014.03.111
0378-7753/

to fossil fuel energy. Biohydrogen production *via* dark fermentation (DF) has garnered significant focus among the available methods due to its low economics and ease of operation [2]. Biohydrogen production is the initial part of anaerobic digestion (AD) where the organic substrate is biologically converted to volatile fatty acids (VFAs), releasing H_2 as a by-product, through a series of biochemical reactions [2,3]. On the other side, there is a gap in net energy balance for this process due to the greater consumption of heat and electricity compared to that produced as hydrogen. Also, the left over oxidized metabolites, i.e. VFAs and alcohols, in the DF effluent has a high stored energy values and carbon residues which impede the treatment process of this effluent [2,4,5].

The trend of industrial biotechnology to treat wastes and residues for landfill disposal was switched to direct valorisation to valuable materials and energy, as a result of economic concerns and the increasing concern about low availability of raw materials [6]. Moreover, the high energy consumed by traditional wastewater treatment technologies drive the demand for alternative and effective systems that can also fulfil the energy gap, by its ability to produce clean and sustainable energy while assimilation of wastewater simultaneously [7,8].

In these circumstances, development of processes for the effective utilization of wastewater to generate sustainable energy gained attention of the research fraternity across the globe. Microbial fuel cell (MFC) is one of these technologies that can transform the substrate chemical energy into electrical one by the metabolic activity of microorganisms [9–11]. The main redox reactions of MFC include the oxidation of substrate by anodic microorganisms to produce electrons and protons, in which electrons are transferred to the cathode through the external circuit, while protons are exchanged through the proton exchange membrane (PEM) separating the anode and cathode compartments [10,12]. A wide range of wastewaters have been utilized as anodic fuels in MFC for the power generation as well as their valorization [13]. However, the coulombic and energy conversion efficiencies are lower in these systems due to different electron losses [14–16]. In this context, some researchers started working on integration of multiple bioenergy systems for various forms of energy generation, which is considered more viable than single bioenergy system in terms of energy losses and substrate utilization. In this direction, secondary integration to acidogenic dark fermentation process gained more interest because the fermentation process simplify the complex substrates into simple volatile acids which can be further converted to various value-added products. The short chain fatty acids are energy rich flexible central commodities of bacterial metabolism and can be converted to diverse value added products by altering the bioprocess [17,18]. Integration of photo fermentation for H_2 production [4,19], microalgae growth for lipid production [20], microaerophilic fermentation for bioplastics production [21] and MFC for power production [22–26], are some of the known examples. However, the photo fermentation and MFC operation for the utilization of acid rich effluents though studied well in the past has not yet been fully exploited, especially in the directions of energy conversion efficiencies.

In the present study, an attempt was made to utilize the DFE from sucrose fermentation process as substrate for power production in an MFC at increasing OLR. A detailed evaluation of bioelectrochemical and energy conversion parameters as well as wastewater treatment efficiency was carried out. Comparative evaluation of the results with the existing literature was also done.

Table 1
The characteristics and composition of the original wastewater acquired after dark fermentation (DFE).

Characteristics of wastewater	
pH	4.3
COD (mg l^{-1})	16220
Composition of wastewater[a]	
Sucrose	2687.18
Glucose	951.62
Fructose	4566.78
Xylose	26.36
Acetic acid	1862.29
Propionic acid	64.60
Butyric acid	1754.26
Isobutyric acid	43.94
Caproic acid	34.7
Lactic acid	752.3
Ethanol	1554.8
n-Butanol	2.6

[a] All the concentrations are in mg l^{-1}.

2. Materials and methods

2.1. DFE characteristics

DFE was collected from a continuously running dark fermentation bioreactor at VITO, Belgium, for the production of hydrogen using sucrose as the main substrate. The bioreactor had been running for 150 days at various organic loading rates and retention times. When an effluent sample was taken for the MFC tests, the hydraulic retention time (HRT) was 4 h and the OLR was 96 g COD/L d. The chemical oxygen demand (COD) of the collected DFE was 16.2 g L^{-1} which was stored at 4 °C and brought to room temperature prior to use. The collected wastewater had a pH value of 4.3. The composition of the DFE and it's characteristics are represented in Table 1.

2.2. Biocatalyst

The cattle manure was collected from a livestock farm in Boeretang area in Mol, Belgium, and was used as the raw source of inoculum. The manure (100 g) was dissolved in 1 L of PBS under continuous stirring on a magnetic stirrer (500 rpm) for about 4–5 h, with intermittent mixing by a glass rod to avoid the settlement of sludge particles. The sludge was filtered through large porous metal sieve, so that all the larger particles including stones, threads, fibres, grass, etc., were separated and the fine sludge was collected, after which it was mixed with 40 mM sodium acetate and enriched for 48 h (400 rpm; room temperature). The sludge was then re-filtered with small porous metal mesh to collect the finest part of sludge which includes the biocatalyst and was used as inoculum.

2.3. MFC construction

Dual chambered MFC was fabricated using polyvinylidene difluoride (PVDF) material, each chamber with working volume of 0.03 L and operated in sequential batch mode (Fig. 1). The two compartments were separated by ion permeable dense separator consisted of Zirfon®. Carbon cloth (Mast Carbon™, UK) and Vito CORE™ carbon electrodes (both with a projected surface area of 10 cm^2), were used as anode and cathode, respectively. Stainless steel mesh was used as a current collector for anode. Prior to use, the separator and electrodes were pre-treated in PBS as previously described [27]. Ag/AgCl–3 M KCl (+197 mV vs. SHE) was used as reference electrode (Radiometer Analytical, France). The ion permeable separator (Zirfon®) was placed between the working electrode and the counter electrode, in order to prevent interference of gases (O_2 or H_2) which can be produced at the counter electrode during the polarization measurements. Ambient air (21% O_2) was used as catholyte at an overpressure of 5 m bar (g). The DFE was used as the anolyte by diluting in buffer (mg L^{-1}: NH_4Cl (200),

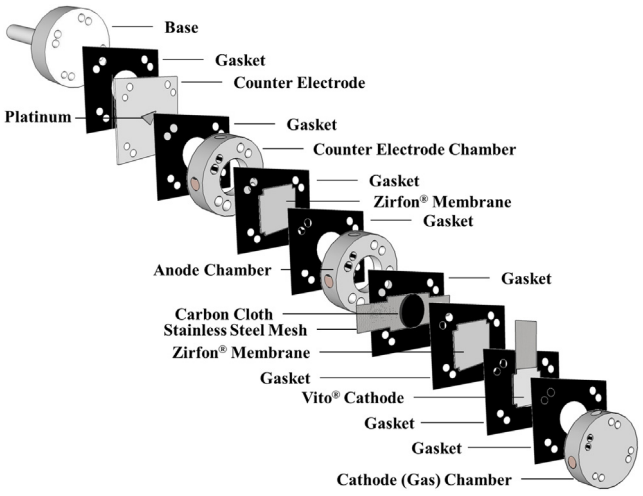

Fig. 1. Schematic representation of MFC design used in the present study.

NaCl (400), $MgCl_2 \cdot 6H_2O$ (200), KH_2PO_4 (500) and yeast extract (10); pH 7) to make up the designate organic loading rate (OLR). MFC was operated at room temperature (22–24 °C). Electrodes were connected externally through concealed copper wire through an external resistance of 1 KΩ, except when stated otherwise. A feed bottle was connected to the anode chamber with silicone tubing, placed with continuous stirring (400 rpm) and nitrogen purging to remove any dissolved oxygen in the substrate. During each feeding event, the electrolyte in the bottle was replaced with the new feed and after 10 min of nitrogen purging allowed to enter into the reactor to make sure of anaerobic environment.

2.4. MFC start-up and operation

The inoculum was brought to room temperature prior to inoculation and then inoculated into the MFC with 5% (v/v) of the anolyte volume. The cell was started up with 10 mM acetate in PBS as electrolyte until the complete development of bacterial biofilm on anode which was indicated by the voltage stabilization. Once the stable voltage was observed in closed circuit mode, the anolyte was switched to DFE diluted in phosphate buffer (PBS) at a rate of 10%, 20% and 30% making a final organic loadings rates (OLR) of 190, 380 and 570 g COD/m^3 day respectively. The pH of the electrolyte was adjusted to 7 and purged with nitrogen prior to feeding every time. The cell was started in open circuit voltage mode (OCV) and after stabilization it was permanently maintained in closed-circuit mode using an external resistance of 1 kΩ. The cell was operated in sequential batch mode, where the electrolyte from the feed bottle was continuously re-circulated through MFC anode using a peristaltic pump (20 mL min^{-1} making a final flow rate of 10 mL min^{-1} in the anode compartment) and was refilled each time after approximately 7 days of retention time.

2.5. Electrochemical analysis and calculations

During start-up, the cell voltage as well as anode and cathode potentials were measured using digital multi-meter. Once the MFC showed stable behaviour, the voltage and current were measured continuously using computer controlled potentiostat (BioLogic-VMP3 model, France) in open and closed circuit modes. Internal resistance of the cell was measured using a milliohm resistance meter (HIOKI 3560 AC mΩ HiTester) during start-up phase. Polarization studies were carried out under varying external load from 10 kΩ to 10 Ω and respective current and power densities were calculated with respect to the anode surface area.

Change in bioelectrocatalytic behaviour of inoculum with change in substrate concentration was studied *in situ* by cyclic voltammetry (CV) using potentiostat linked to a microcomputer data acquisition system during a stabilized phase of operation at each OLR. CV was performed by applying a potential ramp at three different scan rates of 0.5, 5 and 50 mV s^{-1} over the potential range from +0.6 to −0.9 V. All electrochemical assays were performed *in situ* in MFC by considering anode as working electrode and cathode as counter electrode against Ag/AgCl (3 M KCl) reference electrode.

The Coulombic Efficiency (CE) was calculated by integrating the measured current over time relative to the maximum current possible based on the observed COD removal (Eq. (1)) [14].

$$\mathrm{CE} = \frac{M\int_0^t I\mathrm{d}t}{Fbv_{\mathrm{an}}\Delta\mathrm{COD}} \tag{1}$$

where M is the molecular weight of oxygen (32 g), F is the Faraday's constant, b is the number of electrons exchanged per mole of oxygen (4 electrons), v_{an} is the volume of liquid in the anode compartment and ΔCOD is the change in COD over time 't'.

2.6. Bioprocess monitoring

Change in MFC bioprocess was also monitored at regular time intervals in terms of pH, conductivity, soluble COD and composition of waste. The anolyte was sampled once in a week and analysed for soluble COD concentrations, conductivity and pH according to the standard methods [28]. VFAs were monitored in the collected samples using gas chromatograph (GC) (CE Instruments-Thermoquest) equipped with a flame ionization detector (FID) and a 15 m AT-1000 filled capillary column (5.3 μm × 1.2 μm). Helium was used as the carrier gas at a constant flow of 6 mL min^{-1}. The sugars present in the samples were analysed using High performance anion exchange chromatography with pulsed amperometric detection (HPAEC-PAD) system (Dionex ICS-5000) equipped with ED-5000 electrochemical detector. The column used in this system is Carbopac PA -1 (250 mm × 4 mm) coupled to a Carbopac PA-1 (50 mm × 4 mm) guard column. Gradients used in this method includes deionized water (Eluent A and D), 250 mM sodium hydroxide (Eluent B) and 1 M sodium acetate (Eluent C). The flow rate was 1 mL min^{-1}. The elution conditions were varied for detecting monosaccharides and oligosaccharides with a time intervals of 46 min and 100 min respectively. Standard solutions were prepared in the range of 10 ppm–1000 ppm separately for both the methods.

The OLR, substrate degradation rate (SDR) and COD removal efficiency (ξ_{COD}) were calculated using Equations (2) and (3) and 4, respectively.

$$\mathrm{OLR} = \frac{C_{\mathrm{SO}} \times F_{\mathrm{R}}}{R_{\mathrm{v}}} \tag{2}$$

$$\mathrm{SDR} = \frac{(C_{\mathrm{S0}} - C_{\mathrm{S}}) \times F_{\mathrm{R}}}{R_{\mathrm{v}}} \tag{3}$$

$$\xi_{\mathrm{COD}} = \frac{C_{\mathrm{S0}} - C_{\mathrm{S}}}{C_{\mathrm{S0}}} \times 100 \tag{4}$$

where, C_{SO} represents the initial COD concentration (kg m^{-3}) in the feed and C_{S} denotes COD concentration (kg m^{-3}) at defined time. F_{R} represents feed rate (m^3 day^{-1}) and R_{v} denotes reactor volume (m^3).

3. Results and discussions

3.1. Start-up of MFC and stabilization

Initially, the MFC was operated with acetate at an OLR of 100 g COD/m^3 day in open circuit mode. Immediately after feeding acetate and inoculation, the MFC showed anode, cathode and cell potentials of −187 mV, 296 mV and 109 mV respectively. The anode potential increased gradually thereafter and stabilized during first 15 days (∼−534 mV) and the cathode potential was more or less stable (∼242 mV). In response to the increasing anode potential, the net cell voltage also steadily increased during first 26 days and recorded highest OCV (780 mV). The adaptation phase of the mixed culture continued for the first 15 days with slow increment in the cell voltage, due to the lag phase of the inoculum (accounting for 2–3 cycles) in discharging the electrons to the exterior environment [29,30]. Surprisingly, this was also accompanied by the increase in internal resistance from 14 Ω to 21 Ω in 26 days which may be due to the biofilm formation on the anode and the acetate degradation. The pH of the anode chamber was in the range of 7.3–7.8 during 3 cycles of adaptation in the open circuit mode. The voltage stabilization was increased with each feed replacement supporting the adaptation tendency of the inoculum to the electrogenic environment.

After reaching the maximum OCV, the cell was switched to the closed circuit mode with external load of 1 KΩ and operated for 2 feeding events. A rapid drop in cell potential was observed immediately after closing the circuit (528 mV) and continued gradually during first 3 days to reach 140 mV. Thereafter, the voltage was stable and increased steadily to reach 360 mV in 8 days with simultaneous increment in current output from 0.13 mA to 0.36 mA. MFC was operated in closed circuit mode (1 kΩ) for about 65 days, with acetate as the substrate for 11 days and with DFE as substrate at different OLRs for 54 days. After adapting the inoculum to the closed circuit mode, the acetate was replaced with 10% DFE (OLR I, 190 g COD/m^3 day) in PBS and operation was continued.

3.2. Shift in MFC performance with DFE

3.2.1. Electrogenesis and cell design point

Immediately after switching the substrate from acetate to DFE, the voltage showed a gradual drop till 15th day of operation (4th day after feeding DFE) followed by a sharp drop in the cell potential. This was followed by large fluctuations in cell voltage (21–779 mV) for about 6 days (immediately after 2nd feeding event) which may be due to the sharp drop in pH (<4.5). The pH of the DFE was adjusted and then the voltage was stabilized and showed a marginal increment. Similarly, after the next feed change event (26th day of operation), there was again a fluctuation in voltage due to the pH drop. However, this time it was comparatively small change which was stabilized after adjusting the pH. A similar drop was observed for the third time also (33rd day of operation) but after this, the voltage showed a rapid increment and followed by gradual increments in cell voltage. The voltage reached a maximum of 406 mV which is more or less stable for about 5 days indicating the stable phase of operation. A maximum power density of 165 mW m^{-2} was observed after approximately 32 days (4 feeding events) of switching to DFE and was stable for the next 5 days (Fig. 2; Table 2). After detailed evaluation at OLR I, the strength of the DFE was doubled to 380 g COD/m^3 day (OLR II), after which the voltage dropped rapidly and was followed by an increase reaching maximum of 265 mV which contributed to a power density of 86 mW m^{-2}. Similar performance was repeated during second feeding event at OLR II also with a stable power density for about 3 days. When the OLR was tripled (570 g COD/m^3 day), cell voltage depicted similar declining trend likewise with OLR II and stabilized at 197 mV contributing to a power density of 39 mW m^{-2}. There was no change in cell voltage and power density with a second feeding event also which clearly illustrated the negative effect of the amplified substrate load on the MFC performance. The power density declined by 50% while doubling the organic load (OLR II), and continued decreasing upon the further increase in substrate (OLR III). The volumetric power density (with respect to anodic volume), also showed a higher value at OLR I (6.6 W m^{-3}) followed by OLR II (3.47 W m^{-3}) and OLR III (1.59 W m^{-3}).

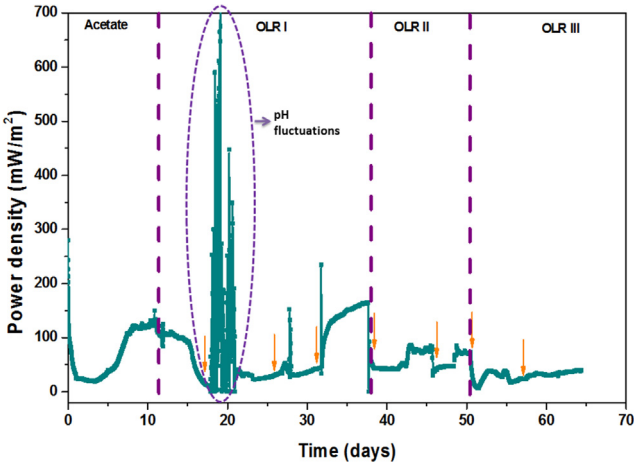

Fig. 2. Change in power density (mW m^{-2}) in closed circuit mode (1 kΩ) operation with respect to the substrate and loading rates.

3.2.2. Potential losses and cell design point

Polarization study was carried out under varying external loads (10 KΩ to 10 Ω) at each OLR to find out the potential losses and cell design point of the MFC. The change in power density with respect to varying external load was plotted against current density and voltage (Fig. 3).

During polarization, one has to wait till almost constant potential was observed at each external resistance which can be considered as steady state of MFC operation where the current generation is sustainable with negligible potential drop [16]. The point where both the external and internal resistances get equalized, the electron

Table 2
Consolidated data pertaining to the experimental output.

		OLR I	OLR II	OLR III
Cell voltage across 1 kΩ resistance (mV)		406	265	197
Power density (mW m^{-2})		165.03	86.67	39.85
ξ_{COD} (%)		72	40	29
OLR (g COD/m^3 day)		190	380	570
SDR (g COD_R/m^3 day)		140	150	170
Specific power yield (KWh kg COD_R)		0.331	0.159	0.041
Coulombic efficiency (%)		47.82	28.76	5.30
Total charge (C) [measured during CV at 5 mV s^{-1})		4499.06	2539.71	1727.97
Energy conversion (J)		6748.5	3808.5	2590.5
Faradaic current (mA)	Oxidation	4.09	3.24	1.79
	Reduction	−2.09	−2.49	−1.35
Tafel's slope (mV dec^{-1})	Oxidation (β_a)	733.2	762.2	101.6
	Reduction (β_c)	282.7	442.1	297.9
Electron transfer co-efficient	Oxidation (α_a)	2.74×10^{-20}	4.48×10^{-20}	8.36×10^{-21}
	Reduction (α_c)	3.87×10^{-20}	3.63×10^{-20}	4.09×10^{-20}
Polarization resistance R_p (Ω)		273	302	518

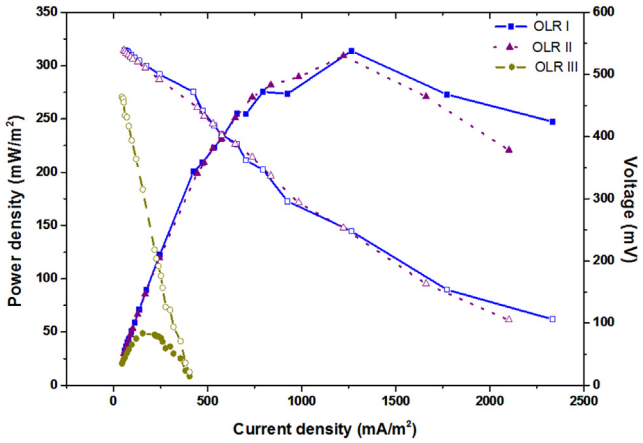

Fig. 3. Polarization behaviour of MFC under varying external load (10 Ω–10 kΩ) depicting the change in power density against current density and voltage with the function of OLR.

discharge from biocatalyst will be sustained for extended periods [31]. Gradual drop in cell voltage was observed at higher resistances, while a rapid drop was observed at lower resistances. After removing the external load, rapid stabilization was observed at higher resistances, while the stabilization was slow at lower resistances indicating typical fuel cell behaviour. At lower resistances, irrespective of the OLR, the voltage sharply declined initially due to the slow redox reactions at the anode surface which led to charge transfer losses followed by a gradual decrease associated with increasing current due to the ohmic losses caused by ionic resistances of all electric circuit elements [14,16]. Though, there is variation in the efficiencies, OLR I and OLR II depicted almost similar electron discharge pattern during polarization. The visible shift in electron discharge was observed at 1 kΩ resistance for OLR I (0.245 mA–0.425 mA) and OLR II (0.243 mA–0.445 mA), while OLR III did not showed any incremental shift in current density throughout the series of external loads. The lower substrate degradation and the associated electron losses might be the reason for the same. For an effective MFC performance, there is a need for optimal anode and cathode potentials satisfying both the cell growth and energy output contributing to higher cell voltages and current densities [29]. The observed higher cell voltage associated with current density contributing to higher power densities at OLR I & II, strongly supports the effective biocatalyst growth and electrogenic activity.

MFC has shown typical fuel cell behaviour at all the three OLRs through increasing power density with decreasing resistance up to a certain point followed by a drop. The resistance at which maximum power density was observed is considered as cell design point (CDP) and the fuel cell can be effectively operated above the cell design point due to the elimination of sharp voltage drops [14,31]. OLR I and II showed a CDP at 200 Ω resistance with varying power densities. OLR I showed higher power density at CDP (313.72 mW m^{-2}), while OLR II showed slightly lower power density (309.66 mW m^{-2}). Surprisingly, OLR III showed CDP at 2 kΩ resistance with comparatively very low power density (48.82 mW m^{-2}). Similarly, under resistances below the CDP, the electron discharge was controlled mostly by the internal resistances contributing to higher current densities associated with voltage drop. At CDP, both the external and internal resistances will collectively lower their influence on the system contributing for higher power densities [16]. In the case of OLR III, the internal resistances might have increased due to higher loads of diverse metabolites and their associated cross-reactions (electron quenching) resulting in CDP at higher resistances with lower power density.

3.3. Bioprocess evaluation

3.3.1. Substrate degradation and conversion efficiencies

MFC has been well established for the complex wastewater treatment with simultaneous power generation [13,32–34]. However, relatively less effort has been put forward in integrating the MFC as secondary treatment unit for the effluents coming from the dark fermentation process to increase the substrate valorization [22–26,35–37]. The wastewater used in the current study was from an operating dark fermentation bioreactor for hydrogen (H_2) production. In general, the effluents of hydrogen bioreactor contains higher quantities of VFA which could be further oxidized at MFC anode for power generation. However, the effluent obtained in the current study contains only 23% of VFA along with several other sugar and alcohol contents (about 89% of the total waste was identified). The detailed composition of the wastewater is depicted in Table 1, comprising 17% of sucrose, 28% of fructose and 10% of ethanol as major fractions. 15% of substrate (2850 g m^{-3} of COD) was removed during first stage of experiment (H_2 production process) in 4 h of retention time associated with a total H_2 production of 7.57 mol. The residual carbon source comprising a diverse metabolite profile was used as substrate in MFC. Detailed investigation of the outlet from MFC has revealed several interesting facts related to the shifts in sugars concentrations (Table 3) that can be well correlated with the shifts in bioprocess. The concentration of fructose was higher compared to others in the effluent collected from the fermentation resulting from the initial hydrolysis of sucrose to its respective monomers. Consequently, the biocatalyst in the first stage might have utilized glucose preferentially and hence its concentrations are lower than the others. Negligible amounts of xylose also present in the effluent and it showed increment by the end of cycle at each OLR indicating the possibility of other sugar metabolisms. The glucose and fructose disappeared after 7 days of MFC operation, even at higher OLR, indicating their consumption by the biocatalyst which was also reflected in increased VFA (Table 3).

The substrate degradation and its energy conversion efficiencies during MFC operation were measured in terms of change in COD. The efficiency of COD removal (ξ_{COD}) and substrate degradation rates (SDR) were calculated and correlated with the power output parameters (Table 2). OLR I has shown higher ξ_{COD} (72%) with an SDR of 140 g COD_R/m^3 day, followed by OLR II (59% and 170 g COD_R/m^3 day) and OLR III (28% and 190 g COD_R/m^3 day). The ξ_{COD} decreased with increasing OLR, while the SDR showed an increasing

Table 3
Shifts in acid metabolites and sugars concentration (in mg l^{-1}) during MFC operation under three OLRs studied.

	Control	OLR I		OLR II		OLR III	
		Inlet	Outlet	Inlet	Outlet	Inlet	Outlet
Organic acids							
Acetic acid	1862.29	281.02	266.66	528.61	487.93	655.31	524.73
Butyric acid	1754.26	174.93	98.61	265.99	387.80	507.31	828.27
Isobutyric acid	43.94	13.41	28.25	20.15	22.96	24.95	59.02
Propionic acid	64.60	18.92	4.44	51.02	46.95	39.15	44.37
Valeric acid	–	–	7.23	–	22.81	–	22.15
Isovaleric acid	–	–	5.68	–	4.74	–	8.19
Caproic acid	19.44	2.56	5.99	4.25	11.21	6.78	12.36
Isocaproic acid	–	–	0.59	–	76.80	–	148.04
Total VFA	3744.27	553.23	462.45	902.6	1049.99	1273.68	1634.77
Sugars							
Sucrose	2687.18	272.26	95.94	546.82	281.34	827.39	407.42
Glucose	951.62	95.84	–	196.43	–	294.65	–
Fructose	4566.78	462.81	–	926.58	–	1397.22	–
Xylose	26.36	3.44	10.84	5.84	15.96	8.21	17.78
Total sugars	8231.94	834.35	106.78	1675.67	297.30	2527.47	425.20

trend indicating that the biodegradation efficiency was decreased with increasing OLR. This might be attributed to the increasing concentration of substrate as well as the diverse metabolites. Overall, both the processes have shown a total COD removal of ~24% associated with bioenergy in the form of H_2 and electricity.

The energy conversion efficiency was calculated both in terms of coulombic efficiency and power yields which gave a clear picture of energy conservation during MFC operation. The coulombic efficiency was much higher with OLR I (47.82%), which decreased to almost 50% by doubling the OLR (OLR II, 28.76%). Further increment in OLR showed almost 10 times drop in CE (OLR III, 5.30%), indicating the negative impact of increased concentration of diverse metabolites on the biocatalyst metabolic activities as well as the increased mass transfer limitations.

The specific power yield (SPY) also showed similar type of changes with OLR, depicting higher values at OLR I (0.331 KWh kg COD_R) followed by a 50% drop at OLR II (0.159 KWh kg COD_R) and about 8 times further drop at OLR III (0.041 KWh kg COD_R). It was reported that a MFC can theoretically produce 3 kWh energy from the degradation (considering 100% degradation) of one kg of organic matter, based on the calorific value of glucose [25,38]. However, when it comes to practice, a maximum of 70–80% of this efficiency can be expected when simple organic substrates are used due to various electron losses and substrate nature. In the current study, we were able to achieve higher conversion efficiencies of 11.03% (COD captured as power at OLR I) compared to the reported values for pure acetate and butyrate in literature [37]. The conversion efficiency decreased to 5.3% at OLR II but can also be compared to the reported values. However, further increment in OLR has shown quite lower value of conversion (OLR III, 1.36%) indicating the overload of the substrate on the biocatalyst. If the overall process efficiency was considered, ~0.83 KWh energy production was observed (considering energy from H_2 @ rate of 0.065 KWh) in the case of OLR I which increases the valorization of the waste. When back calculated from the energy conversion, the possible moles of methane which could generate this much energy are about 3.35 mol (based on 890 KJ of heat energy per 1 mol of CH_4) from ~24% of COD conversion. Henceforth, the integrated process could be compared with the conventional anaerobic digestion for methane production in terms of energy, at the same substrate removal efficiency. However, the substrate degradation would typically be much higher in the latter case, particularly on these type of substrates. MFC technology has still a long way to go to become a mature technology but the anaerobic digestion is already a grown-up one and hence, these results cannot be fully compared with the anaerobic digestion.

3.3.2. Shifts in system redox condition

VFA and pH are the integral expressions of the acid–base conditions of any anaerobic process as well as intrinsic index of the shifts in the bioprocess [31]. Fermentative substrate conversion is generally associated with the generation of acids and solvents as metabolic intermediates due to the acidogenic metabolism. However, when the effluents from hydrogen bioreactor were considered as substrates in MFC, both the conversion of organic fraction to metabolic intermediates and their simultaneous conversion to end products (such as CO_2) will determine the shifts in bioprocess.

The shifts in system redox state was expressed in terms of pH, which showed a diverse pattern with respect to the substrate nature and loading rate (Fig 4). Initially during acetate oxidation, the pH did not vary much (7.4 ± 0.4) and showed increment witnessing the acetate oxidation but once the DFE was loaded, the pH showed a large variations. After loading DFE at OLR I, the pH dropped till below 6.0 indicating the oxidation of sugars producing VFA but not oxidizing the acids. Immediately after feeding second cycle, the pH drop continued till 5.4 reflecting the fluctuations in power density. The pH of the system was re-adjusted to ~7.0 but it dropped again till below 6.0 and the drop continued till the end of cycle. After feeding third cycle also, pH showed decrement immediately but the fluctuations in power were reduced indicating the adaptation of biocatalyst to the new environment. The pH was adjusted here also which dropped gradually to 5.96 at the end of cycle and new feed was replaced adjusting the pH. After the feed was replaced and the pH was re-adjusted to 7.0 a positive shift in pH towards neutral was observed during this cycle which continued to more basic pH (8.6) indicating the shift in redox process. System redox state (pH) has significant impact on the power generation efficiency of MFC due to the change in proton (H^+) shuttling and electron (e^-) discharge phenomenon [33]. The observed fluctuations in the power density strongly support this behaviour. After first pH adjustment, the pH drop was reduced and with further adjustments, it completely disappeared with simultaneous power shoot-up which stabilized at more or less similar value for about 5 days. Higher cell voltage and power density recorded after these pH adjustments support the same. However, the system pH at OLR II and OLR III also dropped with time during operation, even in two cycles, but there are no fluctuations in the power output witnessing the biocatalyst adaptation towards utilizing the sugars as well as VFA for power generation.

The DFE itself is acidic in nature due to the presence of acid intermediates as well as high amount of fructose (ketone functional group), which hinders the effective biological treatment. The negative impact of highly acidic pH on power generation was reported in various studies [39,40], which was also supported by the current study. The biocatalyst was enriched with acetate as sole substrate and during its oxidation, the bicarbonate is produced which does not affect the pH. When the DFE with diverse metabolic intermediates and carbon source was fed to the MFC, the biocatalyst may not be able to adjust to the new redox environment resulting in fluctuations of pH and in turn the power density. Similarly, when the organic load was increased to OLR II and OLR III, the pH showed a drop but there were no fluctuations in the power output observed. The adaptation of the biocatalyst to the new substrate might be the possible reason for this.

The qualitative analysis of organic acid composition was also carried out for both the initial and final samples from the MFC at each OLR along with the initial raw effluent collected from dark fermentation to see the shifts in metabolite concentrations and depicted in Table 3. The initial effluent consisted of 3744 mg L^{-1} concentration of total VFA contributing to about 23% of the COD. The

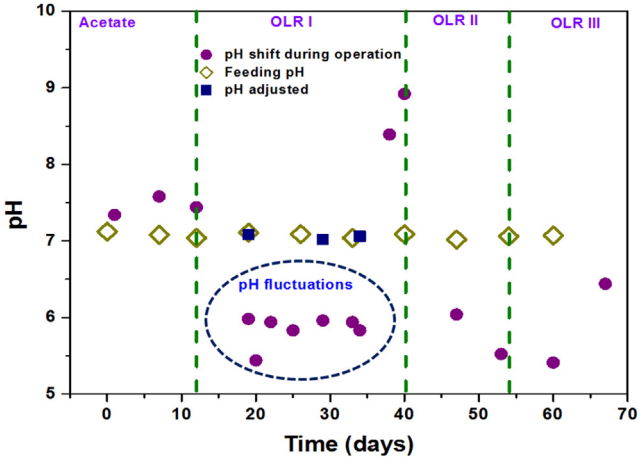

Fig. 4. Shifts in system redox state (pH) with respect to the change in substrate concentration and operation time.

remaining 67% is mostly comprised of sugars and alcohols. Major fraction of VFA was occupied by acetate and butyrate but the other organic acids were also present in very low quantities. During MFC operation, significant variation was observed in the concentrations of acetate and butyrate irrespective of the OLR when compared to the other organic acids. Interestingly, the substrate degradation was not completely reflected in organic acid removal due to the simultaneous generation of organic acids from the sugar components of DFE. Though, the substrate degradation was higher with the OLR I, the VFA removal was very low. When the loading rate was increased, the VFA concentration even increased from inlet to the outlet. Moreover, the diversity of organic acids increased compared to the original effluent. This type of behaviour was also observed in the previous study of authors, where the VFA concentration showed increment with time of operation [41]. The propionate concentration in the DFE could also be contributed for the power generation effectively because it was reported that propionate at concentrations of about 20 mg L^{-1}, will also increase the power densities of MFC [42]. In the current study, the propionate concentrations are higher and showed degradation with time, especially at OLR I, which might also have contributed for higher power densities.

3.4. Bioelectrochemical evaluation

Bioelectrochemical shifts during MFC operation were studied at each OLR under steady state conditions in terms of cyclic voltammetry (CV). CV helps to detect the redox signals and permits the elucidation of possible oxidation and reduction reactions happening at the solution electrode interface and the electrochemical reactions occurring at the electrode surface [16,43]. Reducing equivalents [protons (H^+) and electrons (e^-)] generated from the biocatalyst metabolic activities will move towards the working electrode under applied potential generating a Voltammogram. Voltammograms (vs Ag/AgCl) visualized marked variation in the electron discharge pattern and energy conversion efficiencies with the function of OLR (Fig. 5).

3.4.1. Faradaic currents

Irrespective of the OLR, the oxidation currents were higher than reduction indicating the more efficient anodic biocatalyst metabolism. The shifts in reduction current were very low compared to oxidation with OLR indicating the almost similar cathodic reduction reaction. However, the variation among the oxidation and reduction currents decreased with increasing OLR which might be due to the increasing interference reactions in MFC restricting the flow of reducing equivalents (kinetic/mass transfer limitations). The gas-diffusion electrode, proprietary material of VITO (VITO CoRE™ electrodes) facilitates the contact between the anolyte and gas making the reducing equivalents available for the reduction in presence of the terminal electron acceptor (TEA; oxygen). However, the cathode is not physically separated from the anolyte which facilitates higher interference reactions at cathode also, especially at higher loading rates due to the increased concentrations of diverse metabolites.

Slight variation in the redox currents were observed when shifted from OLR I to OLR II but the variation was significant when the DFE was shifted to OLR III. The faradaic current during oxidation sweep was decreased from OLR I (−4.09 mA) to OLR II (−3.24 mA). On the contrary, the reduction currents were slightly increased from OLR I (2.09 mA) to OLR II (2.49 mA) indicating the increased reduction reaction. When the substrate concentration was further increased (OLR III), both the oxidation and reduction currents (1.79 mA and −1.35 mA) showed a significant drop which might be due to the negative effects caused by the increased concentrations of unwanted diverse metabolites of the wastewater. Clear redox

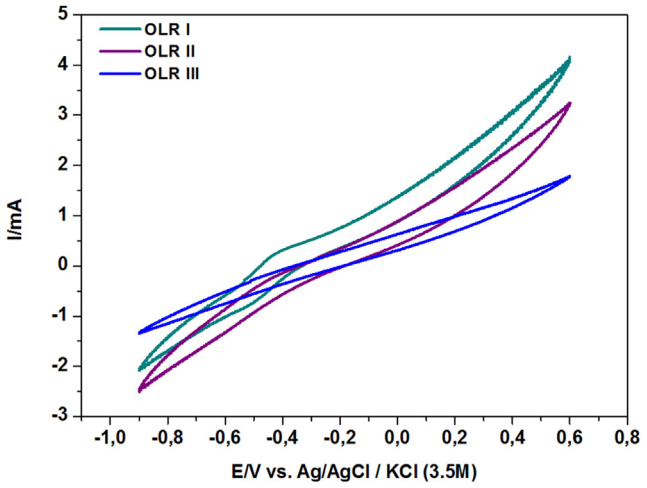

Fig. 5. Change in bioelectrochemical behaviour of the biocatalyst with respect to the change in OLR, in terms of cyclic voltammogram [anode and cathode as working and counter electrodes against Ag/AgCl (3.5 KCl) reference electrode; 5 mV s^{-1} scan rate].

peaks were not observed on the voltammetric signature in the range of applied potential due to *in situ* measurement using anode as working electrode instead of using noble metal electrodes having higher electrochemical properties and due to the usage of wastewater as electrolyte. The number of electrons (e^-) present in the system in the range of applied potential is called charge (Q), which can be converted to energy (W) by using the relation $W = V_{max} \times Q$, where, V_{max} is maximum voltage and Q is the total charge obtained from the respective voltammogram. The electron discharge is directly proportional to the energy (W) obtained during the MFC operation and gives information about the rate of metabolic activities which can also be further correlated with the substrate degradation. The charge depicted a high value (4499 C) at OLR I contributing to an estimated energy of 6748 J, which decreased to almost half at OLR II (2539 C and 3808 J) and further lowered at OLR III (1727 C and 2590 J).

3.4.2. Redox Tafel slopes

The bioelectrochemical evaluation was further extended using Tafel slope analysis to find out the losses and resistance for the electron flow (Table 2). Tafel analysis is the derived kinetics of voltammogram which provides a visual understanding of the shifts in the oxidation and reduction reactions along with the losses present in the system that helps to interpret the biocatalytic activity [16]. The semi-empirical Tafel equation (Eqs. (5) and (6)) can be expressed by

$$\ln i = i_0 + \propto_a nFE/RT \quad (5)$$

$$\ln i = i_0 - \propto_c nFE/RT \quad (6)$$

where, i represents current (A), E is applied voltage (V), β_a ($\alpha_a\, nFE/RT$) and β_c ($\alpha_c\, nFE/RT$) represents oxidative and reductive Tafel slopes respectively, R is the gas constant (8.314 J mol^{-1} K), T is the temperature in Kelvin (298), n is the number of electrons transferred at the rate limiting step and F is the Faraday's constant (96,485). These equations simplify the kinetics of electron transfer controlled process to redox Tafel slopes (β_a and β_c) which are inversely proportional to the process. Tafel analysis also helps to express the electron transfer resistances in terms of the polarization resistance (R_p, Ω). The redox Tafel slopes are inversely proportional to the actual process, which means higher the Tafel slope, lower the oxidation or reduction

process happening on the electrode surface. The oxidative Tafel slope showed a marginal increment from OLR I (733.2 mV dec^{-1}) to OLR II (762.2 mV dec^{-1}), while the reduction slope increased significantly from 282.7 mV dec^{-1} to 442.1 mV dec^{-1}. This shows the similar rate of substrate oxidation to generate the reducing equivalents but the reduction reaction at cathode was decreased which may be due to the kinetic/mass transfer limitations.

Higher oxidative current and low reduction currents during CV along with the higher SDR observed with OLR II also supports this observation. Contrary to the other parameters, both the redox Tafel slopes showed a significant decrement (101.6 mV dec^{-1} and 297.9 mV dec^{-1}) with increasing the substrate to OLR III. This might be attributed to the increased substrate oxidation as well as the reduction of generated reducing equivalents. However, the interference reactions including the mass transfer limitations and electron quenching might be contributing in lower catalytic currents in CV and power outputs. Increased SDR with OLR III supports the same. This behaviour of biocatalyst is suggesting the increment in the degradation rate of organic matter with increasing OLR but not on relative rates. Moreover, the increased concentrations of metabolites might also switch the alternate pathways contributing to the electron losses. Increased polarization resistance with increasing OLR (OLR I: 273 Ω; OLR II: 302 Ω; OLR III: 518 Ω) strongly indicates the increasing internal resistances as indicated above.

Further, the simple charge transfer reactions can be exploited by the linear portion of Tafel slope for deriving the number of electrons transferred in the process. The electron transfer coefficient (α) describe the symmetry between the forward and reverse electron transfer steps, according to the Butler–Volmer model of electrode kinetics which can be calculated by $\alpha_a = \beta_a RT/nF$ and $\alpha_c = \beta_c RT/nF$. The electron transfer co-efficient indicates the energy required for the electron mobility between the biocatalyst and anode and hence it is inversely proportional to the electron transfer rate. Lower electron transfer co-efficient indicates less activation energy requirement for the electron transfer incurring for the lower activation losses. Electron transfer coefficient during oxidation (α_a) and reduction (α_c) varied significantly with the function of organic load (Table 2). The electron transfer co-efficient supported the observed redox Tafel slopes. Negligible variation in the electron transfer co-efficient was observed from OLR I (3.87×10^{-20}) to OLR II (3.63×10^{-20}) which was increased with OLR III (4.09×10^{-20}) indicating the increment in the required activation energy for the electron transfer during reduction reaction. On the contrary, the co-efficient during oxidation increased from OLR I (2.74×10^{-20}) to OLR II (4.48×10^{-20}) but decreased significantly from OLR II to OLR III (8.36×10^{-21}) indicating the higher oxidation possibilities at OLR III. In conclusion, the bio-electrochemical evaluation depicted that the increment in OLR has resulted in higher substrate oxidation but due to the hindering internal electron losses, the power output was significantly reduced.

3.5. Comparative evaluation of the MFC performance

There are some studies reported in the literature based on utilizing organic acids (pure/mixed) and effluents from different processes as primary substrates for the power generation in MFC. Table 4 depicts the comparative MFC performances in various studies reported. All these studies vary in configuration, substrate load, electrode materials and surface area, cathode and TEA, etc. We tried to project the equalized data pertaining to the volumetric power density (based on anode net volume), substrate degradation rate and efficiency, coulombic efficiency and fraction of substrate converted to power. All these studies were carried out in a membrane based single/dual chambered fuel cell configurations.

The conversion efficiencies of the system were similar to the regular fuel cells, indicating the higher efficiency of this system. All the studies have reported the CE between 12 and 75%, but the studies with real fermentation effluents range only between 12 and 35%. In the current study and our previous study [24], we have reported higher coulombic efficiencies of 48% and 46% respectively. In studies with single and mixed synthetic organic acids, higher CEs (60–75%) were reported [35,36]. However, these two studies used hexacyanoferrate (HCF) as TEA and granular graphite as anode/cathode. In the current study, open air was used as TEA on a simple gas diffusion electrode made of activated carbon as cathode and carbon felt as anode, which shows the higher conversion efficiency. Similarly, the power density and substrate degradation efficiencies were also competent and higher than most of the reported literature with real field fermentation effluents. Alterman and co-workers have reported higher power densities of 58 and 42 W m^{-3} respectively using anaerobic digester influent and effluents as substrates, but were reported at 50–100 Ω resistance [25].

Current study was carried out at 1000 Ω resistance and the reported 12.5 W m^{-3} power density was at cell design point (200 Ω). Relatively higher CEs observed during this study could be attributed to the presence of simple sugars sucrose and fructose at higher concentrations along with the other metabolic intermediates. The biocatalyst was enriched in presence of acetate and is reported to depict higher CEs [35,44] which could effectively oxidize the higher concentrations of acetic and butyric acids contributing for the higher CEs [35,45]. However, the competition between

Table 4
Comparison of MFC performances using different organic acids/fermented effluents as substrates.

Anode/anolyte	Cathode/catholyte	Max. Power density (W m^{-3})	ξ_{COD} (%)	SDR (kg COD_R/m^3 day)	CE (%)	Energy conversion (%)[a]	Reference
Granular graphite matrix/glucose	Granular graphite matrix/HCF	49	–	>0.92	75	25	[36]
Granular graphite matrix/acetate	Granular graphite matrix/HCF	52	–	>1.12	75	25	[36]
Toray carbon paper/acetate	Pt/air	12.7	>99	–	31	7.2	[37]
Toray carbon paper/butyrate	Pt/air	7.6	>98	–	15	5	[37]
Granular graphite/MFA	Granular graphite/HCF	49	39	0.77	61	–	[35]
Graphite/UVW	Graphite/air	0.40	62.86	1.06	–	–	[46]
Graphite/FVW	Graphite/air	1.56	80.00	–	12.59	–	[26]
GF-graphite/ADI	Graphite/HCF	58	–	1.23	20	–	[25]
GF-Graphite/ADE	Graphite/HCF	42	–	2.99	29	–	[25]
Carbon felt/AFWL	Carbon felt/air	0.454	90.97	–	20.27	–	[23]
Graphite fibre brush/PE	Carbon cloth/air	6.9	84	–	18	–	[22]
Graphite fibre brush/FS	Carbon cloth/air	24.3	94	–	33–57	–	[22]
Carbon felt/DFE	VITO cathode/air	0.89	–	–	46	–	[24]
Carbon foam/DFE	VITO cathode/air	12.5	72	0.14	48	11	This work

MFA: mixed fatty acids; UVW: unfermented vegetable waste; FVW: fermented vegetable waste; GF: graphite flakes; ADI: influent of anaerobic digester; ADE: effluent of anaerobic digester; AFWL: acidic food waste leachate; PE: primary effluent; FS: fermented sludge; DFE: dark fermentation effluent; HCF: hexacyanoferrate; Pt: platinum.

[a] Energy conversion efficiency is based on the % COD converted to power.

electroactive, fermentative and other anaerobically respiring organisms for electron donor (electron quenching) might have affected negatively on the CEs [46]. Still the CE observed from this study was quite comparable with the available literature. Mohan and his co-workers [26] also reported an improved fuel cell performance by using the fermented vegetable waste (FVW) instead of unfermented vegetable waste (UVW) with respect to both power output and substrate degradation. It can be concluded from the current study that utilizing the dark fermentation effluents will result in improved energy conversion (both H_2 and electricity) from the waste valorization. The MFC configuration used in the current study is also very much effective with lower economics.

4. Conclusions

An MFC was operated with enriched biocatalyst from farm manure to utilize the dark fermentation effluents for power generation and the bioelectrochemical valorization of organic acids. Higher power output was recorded at OLR I and the efficiency decreased with increasing OLR. The substrate degradation efficiency and energy conversion efficiency also followed the similar pattern. Presence of higher concentrations of fructose and sucrose along with the acetate, butyrate and propionate might be the reason for the observed higher power outputs. The additional carbon source, along with the organic acids and ethanol, resulted in simultaneous VFA production and their oxidation. This has depicted an increment in VFA concentration, in spite of COD removal, especially at higher loading rates.

Cyclic voltammograms showed a clear shift in redox currents with change in OLR. Tafel slopes and polarization resistances were also calculated and were well corroborated with the obtained power outputs. Comparatively higher conversion efficiencies than existing literature were obtained during this study. The output from this study will be further extended with a real-field biorefinery wastewater of higher strength.

Acknowledgements

Part of this work was supported by the European Commission (Water4crops, contract no. 311933, FP7). Dr. Ahmed ElMekawy would like to acknowledge the Egyptian government for the ParOwn grant through which this research was conducted at Flemish Institute for Technological Research (VITO), Belgium. Dr. Sandipam Srikanth gratefully acknowledges the Marie-Curie International Incoming Fellowship (IIF) supported project ELECTRO-ENZEQUEST (Grant No: 330803) from the European Commission.

References

[1] A.K. Shein, State of the climate in 2005, Bull. Am. Meteorol. Soc. (2006).
[2] S. Venkata Mohan, G. Mohanakrishna, S. Srikanth, in: A. Pandey, C. Larroche, S.C. Ricke, C.-G. Dussap, E. Gnansounou (Eds.), Biofuels Altern. Feed. Convers. Process., Academic Press, Imprint of Elsevier, Burlington, 2011, pp. 499–524.
[3] S. Rittmann, C. Herwig, Microb. Cell. Fact. 11 (2012) 115.
[4] S. Srikanth, S. Venkata Mohan, M. Prathima Devi, M. Lenin Babu, P.N. Sarma, Int. J. Hydrogen Energy 34 (2009) 1771.
[5] T. Tommasi, B. Ruggeri, S. Sanfilippo, J. Clean. Prod. 34 (2012) 91.
[6] A. ElMekawy, L. Diels, H. De Wever, D. Pant, Environ. Sci. Technol. 47 (2013) 9014.
[7] R. Faiz, K. Li, Desalination 287 (2012) 82.
[8] M.K. Souhaimi, A.F. Ismail, Desalination 287 (2012) 1.
[9] M. Ghasemi, M. Ismail, S.K. Kamarudin, K. Saeedfar, W.R.W. Daud, S.H.A. Hassan, L.Y. Heng, J. Alam, S.-E. Oh, Appl. Energy 102 (2013) 1050.
[10] Y. Kim, B.E. Logan, Desalination 308 (2013) 115.
[11] S. Sevda, X. Dominguez-Benetton, K. Vanbroekhoven, H. De Wever, T.R. Sreekrishnan, D. Pant, Appl. Energy 105 (2013) 194.
[12] S.-E. Oh, S. Van Ginkel, B.E. Logan, Environ. Sci. Technol. 37 (2003) 5186.
[13] D. Pant, G. Van Bogaert, L. Diels, K. Vanbroekhoven, Bioresour. Technol. 101 (2010) 1533.
[14] B.E. Logan, B. Hamelers, R. Rozendal, U. Schröder, J. Keller, S. Freguia, P. Aelterman, W. Verstraete, K. Rabaey, Environ. Sci. Technol. 40 (2006) 5181.
[15] A. ElMekawy, H.M. Hegab, X. Dominguez-Benetton, D. Pant, Bioresour. Technol. 142 (2013) 672.
[16] S. Srikanth, S. Venkata Mohan, Bioresour. Technol. 123 (2012) 480.
[17] R.R. Singhania, A.K. Patel, G. Christophe, P. Fontanille, C. Larroche, Bioresour. Technol. 145 (2013) 166.
[18] J. Yan, G. Lidén, D. Chiaramonti, Y. Chen, J. Luo, Y. Yan, L. Feng, Appl. Energy 102 (2013) 1197.
[19] S. Srikanth, S. Venkata Mohan, M. Prathima Devi, D. Peri, P.N. Sarma, Int. J. Hydrogen Energy 34 (2009) 7513.
[20] S. Venkata Mohan, M. Prathima Devi, Bioresour. Technol. 123 (2012) 627.
[21] M.V. Reddy, S.V. Mohan, Bioresour. Technol. 103 (2012) 313.
[22] F. Yang, L. Ren, Y. Pu, B.E. Logan, Bioresour. Technol. 128 (2013) 784.
[23] X.M. Li, K.Y. Cheng, A. Selvam, J.W.C. Wong, Process Biochem. 48 (2013) 283.
[24] D. Pant, D. Arslan, G. Van Bogaert, Y.A. Gallego, H. De Wever, L. Diels, K. Vanbroekhoven, Environ. Technol. 34 (2013) 1935.
[25] P. Aelterman, K. Rabaey, P. Clauwaert, W. Verstraete, Water Sci. Technol. 54 (2006) 9.
[26] G. Mohanakrishna, S. Venkata Mohan, P.N. Sarma, Int. J. Hydrogen Energy 35 (2010) 3440.
[27] D. Pant, G. Van Bogaert, M. De Smet, L. Diels, K. Vanbroekhoven, Electrochim. Acta 55 (2010) 7710.
[28] APHA, Standard Methods for the Examination of Water and Wastewater, American Public Health Association/American Water Works Association/Water Environment Federation, Washington DC, USA, 1998.
[29] S. Srikanth, S. Venkata Mohan, P.N. Sarma, Bioresour. Technol. 101 (2010) 5337.
[30] M.M. Mardanpour, M. Nasr Esfahany, T. Behzad, R. Sedaqatvand, Biosens. Bioelectron. 38 (2012) 264.
[31] M.V. Reddy, S. Srikanth, S.V. Mohan, P.N. Sarma, Bioelectrochemistry 77 (2010) 125.
[32] H. Moon, I.S. Chang, B.H. Kim, Bioresour. Technol. 97 (2006) 621.
[33] S.V. Raghavulu, S.V. Mohan, R.K. Goud, P.N. Sarma, Electrochem. Commun. 11 (2009) 371.
[34] S. Venkata Mohan, S. Srikanth, G. Velvizhi, M. Lenin Babu, in: V.K. Gupta, M.G. Tuohy (Eds.), Biofuel Technol. Recent Dev., Springer, 2013.
[35] S. Freguia, E.H. Teh, N. Boon, K.M. Leung, J. Keller, K. Rabaey, Bioresour. Technol. 101 (2010) 1233.
[36] K. Rabaey, P. Clauwaert, P. Aelterman, W. Verstraete, Environ. Sci. Technol. 39 (2005) 8077.
[37] H. Liu, S. Cheng, B.E. Logan, Environ. Sci. Technol. 39 (2005) 658.
[38] K. Rabaey, G. Lissens, W. Verstraete, in: P. Lens, P. Westermann, M. Haberbauer, A. Moreno (Eds.), Biofuels Fuel Cells Renew. Energy from Biomass Ferment., IWA Publishing, 2005, pp. 375–396.
[39] G.-C. Gil, I.-S. Chang, B.-H. Kim, M. Kim, J.-K. Jang, H.S. Park, H.-J. Kim, Biosens. Bioelectron. 18 (2003) 327.
[40] Z. He, S.D. Minteer, L.T. Angenent, Environ. Sci. Technol. 39 (2005) 5262.
[41] S. Sevda, X. Dominguez-Benetton, K. Vanbroekhoven, T.R. Sreekrishnan, D. Pant, Chem. Eng. J. 228 (2013) 1.
[42] A. Kaur, J.R. Kim, I. Michie, R.M. Dinsdale, A.J. Guwy, G.C. Premier, Biosens. Bioelectron. 47 (2013) 50.
[43] S.A. Patil, C. Hägerhäll, L. Gorton, Bioanal. Rev. 4 (2012) 159.
[44] E. Zhang, W. Xu, G. Diao, C. Shuang, J. Power Sources 161 (2006) 820.
[45] S.-X. Teng, Z.-H. Tong, W.-W. Li, S.-G. Wang, G.-P. Sheng, X.-Y. Shi, X.-W. Liu, H.-Q. Yu, Appl. Microbiol. Biotechnol. 87 (2010) 2365.
[46] B.E. Logan, Microbial Fuel Cells, John Wiley & Sons, New York, 2008.